The right ventricle of Tetralogy of Fallot patients undergoing pulmonary valve replacement has normal myofilament function but shows perturbations to the expression of extracellular matrix genes

Accepted in *Journal of the American Heart Association*

Accepted on 28/05/2020

Daniel Brayson, PhD,[1] So-Jin Holohan, PhD;[1] Sonya C Bardswell, PhD;[1] Matthew Arno; PhD,[2] Han Lu, PhD;[2] Hanna K Jensen, MD, PhD;[3] Phan Kiet Tran, MD;[3] Javier Barallobre-Barreiro, PhD;[1] Manuel Mayr, MD, PhD;[1] Cristobal G. dos Remedios, MD, PhD;[4] Victor T. Tsang MD, FRCS,[3] Alessandra Frigiola*, MD, MD(res),[3,5,6] Jonathan C Kentish* MA, PhD.[1]

** These authors contributed equally to this work*

Affiliations:

[1]School of Cardiovascular Medicine and Sciences, King's College London BHF Centre for Research Excellence, London, UK

[2]Genomics Centre, Faculty of Life Sciences and Medicine, King's College London, London, UK

[3]Cardiovascular Directorate, Great Ormond Street Hospital, London, UK

[4]Department of Anatomy, Bosch Institute, University of Sydney, Sydney, NSW, Australia

[5]Cardiovascular Directorate, Guys and St Thomas' NHS Foundation Trust, St Thomas' Hospital, London, UK

[6] School of Biomedical Engineering and Imaging Sciences, Kings College, London, UK

Short Title: *Myofibrils and ECM in RV of rToF patients at time of PVR*

Addresses for correspondence:

Jonathan C Kentish

School of Cardiovascular Medicine and Sciences

The Rayne Institute

4th Floor, Lambeth Wing

St Thomas' Hospital

London SE1 7EH

Tel: +44 7803 206278

Email: jon.kentish@kcl.ac.uk

Alessandra Frigiola

St Thomas' Hospital

Cardiovascular Directorate

LGF, South Wing

London SE1 7EH

Tel: +44/0 20 7188 1082

Email: alessandra.frigiola@gstt.nhs.uk

Abstract

Background – Patients with Tetralogy of Fallot repair (rToF) who are approaching adulthood often exhibit pulmonary valve regurgitation, leading to right ventricle (RV) dilatation and dysfunction. The regurgitation can be corrected by pulmonary valve replacement (PVR) but the optimal surgical timing remains under debate, mainly due to the poorly understood nature of RV remodeling in rToF patients. The goal of the present study was to probe for pathologic molecular, cellular and tissue changes in the myocardium of rToF patients at the time of PVR.

Methods and Results – We measured contractile function of permeabilized myocytes, collagen content of tissue samples, and the expression of mRNA and selected proteins in RV tissue samples from rToF patients undergoing PVR for severe pulmonary valve regurgitation. The data were compared with non-diseased RV tissue from unused donor hearts. Contractile performance and passive stiffness of the myofilaments in permeabilized myocytes were similar between rToF-PVR and RV donor samples, as was collagen content and crosslinking. There was enhanced mRNA expression in the rToF-PVR patients of genes associated with connective tissue diseases and tissue remodeling, including the small leucine-rich proteoglycans asporin, lumican and osteoglycin, although their protein levels were not significantly increased.

Conclusions – RV myofilaments from rToF-PVR patients showed no functional impairment, but the changes in ECM gene expression may indicate the early stages of remodeling. Overall, our study found no evidence for major damage at the cellular and tissue levels in the RV of rToF patients who underwent PVR according to current clinical criteria.

Keywords:

Tetralogy of Fallot; pulmonary valve replacement; myofibril; extracellular matrix; small leucine rich proteoglycan

Non-standard Abbreviations and Acronyms

CMR cardiac magnetic resonance

CPET cardiopulmonary exercise test

ECM extracellular matrix

EDVi end-diastolic volume indexed for body surface area

EF ejection fraction

ESVi end-systolic volume indexed for body surface area

GO gene ontology

GSEA gene set enrichment analysis

LV left ventricle

NYHA New York Heart Association

PVR pulmonary valve replacement

QC quality control

qPCR quantitative polymerase chain reaction

rToF repair of Tetralogy of Fallot

RV right ventricle

RVOT RV outflow tract

SLRP small leucine rich proteoglycan

SV stroke volume

TAPSE tricuspid annular plane systolic excursion

Clinical Perspective

What is new?

- We found that the contractile function of the myofilaments in the right ventricular myocardium of repaired tetralogy of Fallot patients, taken at the time of pulmonary valve replacement (PVR), was similar to that in age-matched donor controls.
- Similarly, the extracellular collagen matrix was similar to that in donor control tissue, but there were subtle changes in gene expression, particularly in small leucine-rich proteoglycans, although these changes were not reproduced at the protein level

What are the clinical implications?

- The optimal timing for PVR in repaired tetralogy of Fallot patients is controversial
- It has been suggested that right ventricular dilation over the years preceding PVR could lead to pathological changes at the tissue and cellular levels that would limit long-term recovery post-PVR
- Our finding of no evidence for myocyte or extracellular matrix remodeling suggests that patients are not exposed to detrimental or irreversible tissue remodeling with current PVR timing guidelines.
- However, the subtle changes in gene expression may be indicate an impending program of myocardial remodeling

Introduction

Tetralogy of Fallot (ToF) is one of the most common congenital heart diseases, accounting for almost 10% of all cardiac malformations.[1] Without surgical intervention only 10-15% of patients survive beyond the age of 20 years. The modern surgical approach for these patients is for a single-stage repair of ToF (rToF) performed during the first few months of life, which has led to excellent long-term survival (>98% survival at 20 years after repair).[2] Nevertheless, residual hemodynamic lesions remain and need to be addressed to avoid long-term detrimental effects. The most common defect is pulmonary regurgitation, which is now recognized to have deleterious effect on global cardiac function, leading to progressive RV dilatation and dysfunction, tricuspid valve regurgitation, exercise intolerance, arrhythmias and sudden death.[3-6] Pulmonary valve replacement (PVR) is therefore often advocated in the lifetime management of these patients. PVR has been shown in numerous studies to induce beneficial remodeling, not only of the RV but also the left ventricle (LV),[7-9] coupled with improvement in patients' symptoms and exercise capacity.[7] However, the optimal timing for PVR is controversial. To date, all commercially-available pulmonary valves, whether surgically or percutaneously implanted, have a limited durability, hence exposing the patients to the need for multiple procedures during their lifetime. While the number of repeat procedures could be reduced by delaying PVR, any delay could also theoretically lead to irreversible changes in RV structure and function, potentially leading to poor long-term recovery in some patients after PVR. The timing of PVR is therefore critical.

In previous studies, we and others demonstrated a post-PVR positive remodeling, characterized by reduction of RV volumes, increase in LV filling and improvement of biventricular systolic function, across a range of ages but the greatest improvement of LV dynamics and exercise capacity was observed in younger patients (< 18 years). On pre-operative CMR and echocardiographic assessment,

the only difference we observed between younger and older patients was a higher pulmonary valve regurgitant fraction in the younger group, which we interpreted to be the result of a more compliant, less "diseased" right ventricle in younger patients.[7] However, this suggestion highlighted a major deficiency in knowledge in this field: very little is known about the nature and extent of the pathological tissue changes that take place in the dilated RV as a result of severe pulmonary valve regurgitation, that is, by the time that PVR is performed, how severe is the cellular and tissue damage in the RV?

Chronic volume-overload of the left ventricle (for example, due to MI or aortic regurgitation) is associated with changes in the passive stiffness and contractile function of myocytes, and in the microarchitecture of the extracellular matrix (ECM), that may either contribute to, or compensate for, the mechanical dysfunction.[10-12] However, it is not known if similar pathologies exist in the volume-overloaded RV myocardium of rToF patients at the time of PVR. Therefore, in this study we sought to assess the contractile properties and passive stiffness of the cardiac myofilaments, and the composition of the ECM, in these PVR patients in order to better understand the functional properties at the cellular level of the dilated right ventricle with significant pulmonary regurgitation. In the long term, an improved understanding of the nature and extent of the maladaptive RV remodeling may help to inform therapeutic strategies and aid clinical decisions regarding the time at which PVR should be performed in individual rToF patients.

Methods

Data availability

The data that support the findings of this study are available from the corresponding authors upon reasonable request. The microarray data are publicly accessible at the NCBI Gene Expression Omnibus (GEO) database (https://www.ncbi.nlm.nih.gov/geo/) under accession number GSE141955.

Ethical approval

The project was approved by the UK National Research Ethics Committee (Rec #11/LO/1924) and by the local R&D committees of University College London Hospitals, Great Ormond Street Hospital, and Guy's and St Thomas's NHS Foundation Trust. Patients or their legal guardians (as appropriate) were approached at the time of pre-surgical assessment by one of the research fellows (HAJ and PKT). Signed, informed consent was obtained to allow the excised RV tissue to be retained for experimentation after the removal of residual excessive muscle bundles in the RV out-flow tract (RVOT). Consent was also obtained for the retrospective use of clinical data. To allow comparison with RV samples from non-diseased tissue, we also used frozen samples of RV tissue that had been obtained from 7 unused donor hearts; these were selected so that their gender and age profiles (4 males, 3 females; patient age 28 ± 13 yr.) resembled those of the rToF-PVR patients. These samples were obtained from the Sydney Heart Bank, Australia, with full consent of the patients' representatives and with ethics approval (Protocol no. 2012/2814) from the Human Research Ethics Committee of the University of Sydney.

Clinical Assessments

Eight patients (3 males, 5 females; patient age 24 ± 12 yr.), with previous ToF repair, underwent PVR for increasing RV volumes associated with symptoms of shortness of breath on exertion and/or palpitations (median NYHA class II) in agreement with current clinical indications. As part of their clinical pre-operative assessment, all patients underwent echocardiogram, cardiac magnetic resonance imaging (CMR), and cardio-pulmonary exercise testing (CPET), as described below and previously .[13]

Echocardiography

Standard Doppler echocardiography was performed with a VIVID 7 machine (GE Medical Systems, Milwaukee, WI) equipped with a multi-frequency transducer (3.5 and 5 MHz) as previously described.[7] From the apical view, tricuspid annular plane systolic excursion was obtained from M-mode interrogation of the lateral aspect of the tricuspid valve. From the same apical views, tissue Doppler myocardial velocities were obtained at the RV and LV lateral annulus in order to assess longitudinal function. LV ejection fraction was calculated from the parasternal long axis view using Simpson's formula. The degree of tricuspid valve regurgitation (TR) was assessed qualitatively using color Doppler from the apical four chamber view and from the short axis view; the regurgitation was graded as trivial, mild, moderate or severe according to the Doppler intensity. From the TR jet, the RV systolic pressure was obtained using the Bernoulli equation. Peak velocity gradient across the RVOT was calculated from the maximum velocity obtained from the continuous-wave Doppler signal.[14] Pulmonary valve regurgitation was assessed by Color and Pulsed Doppler interrogation of the pulmonary valve (PHT less than 100 ms), and of the main pulmonary artery and branch pulmonary arteries (presence of reversal flow).

Cardiovascular Magnetic Resonance Imaging

Cardiovascular MR (CMR) was performed with a 1.5-T MR scanner (Avanto, Siemens Medical Systems) using techniques previously described.[7] Assessment of LV and RV volumes was performed by manual segmentation of short-axis cine images at end-diastole and end-systole (Argus; Siemens Medical Systems). End-diastolic and end-systolic volumes were calculated by use of Simpson's rule for each ventricle, and from these volumes, stroke volume (SV) and ejection fraction (EF) were calculated. Arterial blood flow was calculated from phase contrast images by use of a semiautomatic vessel edge-detection algorithm (Argus; Siemens Medical Systems) with operator correction. Pulmonary valve regurgitant fraction was calculated as percent backward flow over forward flow. All volume and flow measurements were indexed for body surface area.

Cardiopulmonary Exercise Testing

Cardiopulmonary exercise testing was performed on an electronically-braked bicycle ergometer (Ergoline 900) with respiratory gas exchange analysis. We used a ramp protocol as previously described.[7] Peak oxygen uptake (peak VO_2), VO_2 at the anaerobic threshold, and ventilatory response to carbon dioxide production (VE/VCO_2 slope) were derived from respiratory gas analysis during maximal exercise testing; VE/VCO_2 slope was measured as the slope for the whole exercise.

Functional studies of human permeabilized cardiac myocytes

We carried out functional studies of the myofilaments within human single permeabilized cardiac myocytes that had been prepared from rToF-PVR tissue and RV donor tissue. Myofilament contractile function was assessed from the following: passive myocyte stiffness (at <10 nmol/L Ca^{2+}, which is below the threshold for Ca^{2+} activation of the myofilaments); force production of the myofilaments

when maximally activated with Ca^{2+} (30 µmol/L Ca^{2+}); maximum rate of force redevelopment after a brief release/restretch of the myocyte during maximal Ca^{2+} activation (which gives information on the rate of actomyosin crossbridge cycling); Ca^{2+} sensitivity of myofilament force production, using a range of Ca^{2+} concentrations (0.1 - 30 µmol/L).

The permeabilized myocytes for these experiments were prepared at 4°C by a modification of the method used previously.[15] A frozen piece of rToF-PVR tissue or donor RV tissue was homogenized for 7-10 s in a 1 ml ground-glass hand homogenizer containing skinning solution (= relaxing solution with 1% Triton-X100; ThermoFisher). Relaxing solution had the following composition (mmol/L): BES 100, K propionate 55, Na_2 phosphocreatine 10, Na_2H_2ATP 6.21 (for $MgATP^{2-}$ = 5), $MgCl_2$ 6.24 (for Mg^{2+} = 1), dithiothreitol 1, EGTA 10 (to maintain the free Ca^{2+} concentration at ~1 nM, pCa 9.0), and protease inhibitors leupeptin 0.001, E64 0.001, and AEBSF 0.25 (all from Sigma-Aldrich); pH 7.1 at 4°C; ionic strength 0.20 mol/L. The homogenate in skinning solution was left on ice for 30 mins for permeabilization of the myocyte membranes, then was transferred into a Protein-LoBind Eppendorf tube (Fisher Scientific) and centrifuged (4000 rpm, 4.5 min). The myocyte pellet was washed three times in relaxing solution (4000 rpm, 4.5 min each time) to remove the Triton X-100. The final myocyte suspension in relaxing solution was then stored on ice.

The experimental protocol was modified slightly from that described previously.[15] A permeabilized myocyte was selected and its ends were glued with UV-setting glue (OA63 adhesive and Opticure LED-200 UV light source, Norland) between pins extending from a force transducer and a high-speed length controller (403A and 315C-I, Aurora Scientific Inc., Ontario, Canada). The mean sarcomere length (SL), measured using an Aurora 600A video analysis system in autocorrelation mode, was set to 2.0 µm. Myocytes were rejected if: the cell was visibly damaged; their end attachments were unstable; the resting sarcomere pattern was unclear or misaligned; the force

during Ca^{2+}-activated contraction was unstable; the resting SL after a contraction was substantially different from that pre-contraction. These criteria, plus the fact that it was difficult to prepare more than a few myocytes from the small amounts of rToF-PVR tissue available, meant that it was impossible to obtain useful data from the same number of myocytes from each patient sample. The numbers of data-yielding myocytes from each donor or patient therefore ranged from one to six (details in Fig. 1 legend).

To measure its passive stiffness, the permeabilized myocyte was bathed in relaxing solution at 15°C and given stretches of 1 s duration and various magnitudes to increase SL from 2.0 µm to within the range 2.1 – 2.3 µm.[15] For the present study, we measured the force increment at the end of a stretch from SL 2.0 µm to 2.3 µm and used this increase in resting force as a measure of myocyte passive stiffness.

To examine the Ca^{2+}-activated contractile performance of the permeabilized myocyte, we then perfused the myocyte with a series of CaEGTA-containing activating solutions of Ca^{2+} 0.1 – 30 µmol/L (pCa 7.0 – 4.5; pH 7.1; 15°C).[15] Once force had developed to a steady level (Fig.1A), the myocyte was subjected to a release/restretch protocol to detach all the attached myosin crossbridges from actin. The subsequent recovery of force, as crossbridges re-attached to actin, was fitted with a single exponential fit and the rate constant of tension recovery (k_{tr}) was used as a measure of crossbridge kinetics. Ca^{2+}-activated force was measured as the total steady force in activating solution minus the preceding passive force (at SL 2.0 µm). The relationship between Ca^{2+}-activated force and Ca^{2+} concentration of the activation solution was fitted with a sigmoidal curve (Hill equation), which was used to calculate the pCa required for 50% activation of force (pCa_{50}).

The sensitivity of these techniques to detect functional changes in myocytes from diseased myocardium has been validated in our previous studies, where we found decreased maximum force

but increased k_{tr} and Ca^{2+} sensitivity in myocytes from hypertrophic cardiomyopathy patients[15] and increased Ca^{2+} sensitivity in myocytes from a dilated cardiomyopathy patient.[16]

Histological quantification of collagen

Cryosections cut from frozen blocks of tissue were subjected to xylene clearance and sequential ethanol treatment. Slides were left in Milli-Q H_2O for 5 min followed by a 30 second incubation in 0.2% phosphomolybdic acid. Slides were rinsed in Milli-Q H_2O and then left in 1% Sirius red solution (to stain for collagen) for 90 min. Slides were washed 2x2 min in acidified Milli-Q H_2O (0.05% acetic acid), incubated for 15 min in Picric acid, rinsed 3 times in Milli-Q H_2O, then dehydrated by sequential ethanol treatment: 25%, 50%, 75%, 96% (1 min each) 100%, (2x3 min) xylene, (2x5 min). Glass coverslips were mounted with DPX (Sigma Aldrich, UK) and allowed to dry overnight. Sections were viewed with a light microscope (Zeiss, Germany) without and with a polarization filter, to identify collagen organization. Images were captured and analyzed using Volocity software (Perkin Elmer).

Microarray gene expression profiling

RNA extraction was performed on LN_2 cooled and pulverized heart tissue samples using Direct-zol™ RNA Miniprep plus kit according to the manufacturer's instructions (Zymo Research Corp., CA, USA). RNA quality was assessed using the Agilent 2100 Bioanalyzer (Agilent Technologies LDA UK Limited, Stockport, United Kingdom) and quantified using the Nanodrop ND-1000 Spectrophotometer (Thermo Fisher Scientific, Wilmington, USA). All seven rToF-PVR and six out of seven RV Donor samples passed quality control (QC) and were subsequently subjected to microarray analysis. The gene expression profiles were determined using the GeneChip Human Transcriptome 2.0 Array (Affymetrix, ThermoFisher Scientific). Single Primer Isothermal Amplified (SPIA) cDNA was

generated using the Ovation Pico WTA System V2 kit (Nugen, AC Leek, The Netherlands) following the manufacturer's instructions. In addition, the SPIA cDNA was subjected to a QC check to assess quality (Agilent 2100 Bioanalyzer) and quantity (Nanodrop ND-1000 Spectrophotometer) in preparation for the next stage. The SPIA cDNA was fragmented and biotin-labeled using the Encore Biotin Module (Nugen) according to the manufacturer's instructions. The fragmented and biotin-labeled cDNA was subjected to a further round of QC checks to assess fragmentation size (Agilent 2100 Bioanalyzer). Hybridization cocktails were prepared from the fragmented labeled-cDNA according to Nugen's recommendations and hybridized to the microarrays at 45°C for 18 hours. The arrays were washed and stained using the wash protocol FS450_0001 recommended for GeneChip Human Transcriptome 2.0 Arrays on the GeneChip Fluidics 450 station. The arrays were scanned using the GeneChip Scanner 3000 7G. CEL files were QC assessed in the Expression Console software package (Affymetrix, ThermoFisher Scientific) by using standard metrics and guidelines for the Affymetrix microarray system. Principle component analysis, hierarchical clustering and gene set enrichment analysis (GSEA) were performed in Qlucore Omics Explorer 3.0 (Qlucore, Lund, Sweden). Alignment and comparison to the Gene Ontology database of biological processes was performed in MetaCore™ (Thompson Reuters), and was used to identify processes and pathways represented by the differentially regulated genes. These microarray data have been submitted to NCBI GEO and are accessible through accession number GSE141955

Quantitative PCR

2 µg RNA from the above extraction process was used to synthesize cDNA using an RT^2 First-strand kit (Qiagen). qPCR was carried out using the ΔCt method. 9 µl cDNA was added to 10 µl 2x Sybr green PCR master mix and 5 µmol of forward and reverse primers for the protein of interest (Table

1). Cycling parameters were 94°C for 15 seconds, followed by single-step annealing and extension at 60°C for 1 min (35 cycles). Reactions were carried out in a Corbett RotorGene-3000. The cycle threshold (Ct) was determined automatically by the software and corresponds to a point during the linear phase of amplification. Gene expression of rToF-PVR samples was expressed as fold change compared to RV donor samples, by normalizing individual data points to the mean of RV donors (defined as the control group), which fixed the mean value for the RV donor group to 1.

Extraction of ECM proteins

Tissue was washed in phosphate buffered saline (PBS) and then placed in 0.5 mol/L NaCl extraction buffer (1:10 weight:volume) and shaken (at low speed) for 1 hour at room temperature (RT). Decellularization was then performed in 0.1% SDS, with 25mM EDTA and 1:100 cocktail of protease inhibitors (1:10 weight:volume) and shaken for 18 hours at RT. Finally, samples were added to 4 mol/L guanidine-HCl (1:5 weight:volume) extraction buffer and shaken vigorously for 48 hours at RT to extract the strongly-bound ECM components. Guanidine extracts containing 25µg of protein were subjected to ethanol precipitation at -20^{o}C overnight after adding 10x the volume of ethanol to the extract lysate. Samples were centrifuged at 14,000g for 45 minutes at 4^{o}C. The supernatants were removed and the protein-containing pellets were centrifuged in a vacuum centrifuge for 30 min at 37^{o}C to dry the pellet completely. The pellets were then subjected to complete deglycosylation to remove any glycosaminoglycan chains or N- and O-linked oligosaccharides which might interfere with antibody binding. Deglycosylation was performed by adding to the pellet a deglycosylation buffer (150mM NaCl, 50mM sodium acetate pH6.8, 10mM EDTA and supplemented with protease inhibitors) with enzymes: heparinase (1:500), chondroitinase ABC (1:100), keratinase (1:500) (All Sigma-Aldrich), PNGaseF (1:200), and 3 different debranching enzymes: α2-3,6,8,9-Neuraminidase

(1:200), ß-N-acetylglucosaminidase (1:200) and O-glycosidase for complete removal of O-linked sugars (1:200) (all from Millipore). These were incubated with shaking for 48 hours at 37^{o}C. Sample buffer containing β-mercaptoethanol was added to the deglycosylated samples to a concentration of 0.5 µg/µl in preparation for Western blotting.

Western Blotting

Deglycosylated lysates were heated to 85°C for 10 minutes. A chamber was prepared with a gradient SDS gel of 4-16% acrylamide concentration. 5 µg of 0.5 µg/µl samples were then loaded into each well of the gel. The proteins were separated at 175 mV. Transfer was achieved in wet conditions. The proteins were electrophoretically transferred onto nitrocellulose membranes using 350 mA at RT for 2 hours. Membranes were blocked for 1 hour with 5% Milk in PBS with tween (PBS-T). Primary antibodies were added with PBS-T/5% bovine serum albumin and incubated overnight at 4°C. The membrane was washed 3x15 min with PBS-T. The blots were then incubated in secondary antibody conjugated to HRP for 1 hour. The blots were again washed 3x15 min with PBS-T and bound antibody was detected by ECL detection (GE Healthcare) onto film. Images were scanned and imported to Image Studio Lite (Li-Cor Biosciences) for densitometric analysis.

Immunofluorescence staining

Tissue was removed from storage at -80°C, warmed to -20°C for approximately 1 hour, then mounted onto the stage of a cryostat with OCT compound and allowed to equilibrate to the ambient temperature of the cryostat for 5 min. For cutting tissue, the stage temperature was set to -22°C and the knife was set to -20°C. The sections were then cut to 10 µm thick and mounted onto high quality superfrost slides. The sections were allowed to air dry for approximately 1 hour and then stored at -

80°C. For staining, sections were allowed to dry completely and fixed by immersion, in a coplin jar, in pre-cooled 100% methanol at -20°C for 5 min or 4% formalin for 10 min RT. Sections were washed 2x5 min in PBS, then permeabilized in 0.5% NP-40 for 3 min RT and washed 3x5 min in PBS. Sections were blocked for 1 hour at room temperature in 5% donkey serum. Primary antibody was diluted appropriately in blocking solution, applied to the sections and incubated in a humidified chamber overnight at 4°C. Sections were washed 3x5 min in PBS and secondary antibody conjugated to a fluorophore was diluted as appropriate, applied to the sections and incubated in the dark in a humidified chamber for 1 hour RT. DAPI was added 1:10,000 for 5 min at the end of the incubation for visualization of nucleic structures. Sections were washed 3x5 min in PBS in the dark and then mounted in mowiol mounting media and allowed to dry in the dark overnight. Images were acquired with an A1R point scanning confocal microscope (Nikon)

Antibodies

The antibodies used in this investigation were: Anti-asporin (Thermo Fisher, PA5-13553) polyclonal rabbit IgG, diluted 1:1000 for WB and 1:100 for IF. Anti-collagen I (Abcam, ab90395), monoclonal mouse IgG1, clone COL-1 diluted 1:1000 for IF. Anti-lumican (Santa Cruz, sc-33785), polyclonal rabbit IgG, diluted 1:100 for WB. Anti-Mimecan/Osteoglycin (Abcam, ab110558) polyclonal rabbit IgG, diluted 1:1000 for WB. Anti-myomesin (gift from Elisabeth Ehler), mouse monoclonal IgG, clone B4 diluted 1:100 for IF. In the case of asporin, where band specificity was difficult to determine, we performed sequence alignment of the epitope and discovered homology to biglycan, which has predicted molecular weight ~5 kDa smaller than asporin; we therefore believe the lower band visible on the membrane identifies biglycan. The higher band, we ascribe to incomplete removal of glycosaminoglycans.

Statistical analysis

Results of clinical investigations (CMR, cardiopulmonary exercise testing and echocardiography) were expressed as mean ± SD. Data from functional experiments, qPCR experiments and image analysis of picrosirius red staining were plotted individually and expressed as mean ± SD. Where appropriate, Student's unpaired t-test was applied to test for differences between rToF-PVR and RV Donor groups. For the functional data (force, k_{tr}, pCa_{50}), the data from multiple myocytes were averaged for each patient and the mean value for each patient was taken as a single datum point for the subsequent calculation of overall mean, SD and the t-tests. Because of the technically challenging nature of the work, the number of myocytes per patient/donor was variable (ranging from 1-6). If distribution of the data were not normal, Mann-Whitney test was used, whilst Welch's correction was applied when the variance was unequal between data sets. For transcriptome (mRNA) analysis, two-group comparison with t-test was performed and a threshold *P* value of 0.004 and false discovery rate (q) of 0.47 were selected for principal component analysis and hierarchical clustering. For Gene Ontology enrichment, a hypergeometric test was used with $P < 0.05$ adjusted by Benjamini-Hochberg correction.

Results

Patients' characteristics

Eight patients underwent pulmonary valve replacement, with a mean age of 24 ± 12 years (range 11-49 years). Seven out of eight patients had a trans-annular patch at the time of initial ToF repair and two out of eight patients were previously palliated with a right modified BT shunt. One patient had initial ToF repair with valve preservation (age 3 months) and required subsequent balloon valvotomy (age 9 months) and re-do repair with trans-annular patch (age 10 months). Only two

patients had associated comorbidities; one patient (age 15 years at the time of PVR) suffered from mild right hemiplegia as result of an embolic event at the time of primary repair and had some hearing impairment, whereas another patient (age 11 years at the time of PVR) had a history of high level of consanguinity and presented with IUGR (intra-uterine growth restriction), with associated learning difficulties, bilateral Perthes disease, and eczema. Only one patient (age 49 years) was on medication prior to PVR; medications included betablocker (bisoprolol 1.25mg), aspirin 75mg, and diuretics given only a few weeks before surgery (frusemide 20mg and spironolactone 25mg). Patients' characteristics are summarized in Table 2. All patients had severe pulmonary valve regurgitation (PV RF 48 ± 7%), whereas there was no evidence of significant residual RVOT obstruction (mean RVOT peak velocity 2.2 ± 0.4 m/s). The right ventricle was significantly dilated, with an RV EDVi of 149 ± 26 ml/m^2 and a RV:LV EDVi ratio of 2.2±0.4 but with preserved systolic function (RV EF 56 ± 5%). Left ventricular volumes and systolic function were normal in all (mean LV EDVi 71 ±19ml/m^2, mean EF 66 ± 7%). Two patients had moderate tricuspid regurgitation (TR), 1 patient mild TR, the others trivial or none. Upon cardiopulmonary exercise testing, exercise capacity was found to be only mildly reduced: mean peak VO_2 measured 31 ± 8 ml/min/kg (84 ± 11% of predicted) with a VE/VCO_2 slope of 28 ± 4.

Non-diseased RV tissue samples from 7 unused donor hearts were used as a reference in this study. The donors were selected so that their gender and age profiles (4 males, 3 females; patient age 28 ± 13 yr.) resembled those of the rToF-PVR patients. Five of the seven donors had suffered a subarachnoid hemorrhage after a motor vehicle accident, one donor died from a basal infarct after a grand mal seizure, and one donor died from hypoxia secondary to a seizure. Before explant the hearts were classed as "healthy" but were not used for transplantation owing to lack of a tissue type

match. LV or RV tissue from the same hearts has been used as reference tissue in previous publications by ours and other laboratories.[15, 17-21]

Stiffness and contractile function were similar between permeabilized rToF-PVR and RV donor myocytes

Previous studies have found that in left or right heart failure there are changes in the passive stiffness and Ca^{2+}-activated force development of the cardiac myofilaments (see Discussion); in vivo these alterations would be expected to contribute to diastolic and systolic dysfunction, respectively. We investigated whether similar changes could be observed with the myofilaments from the right ventricles of the rToF-PVR patients by measuring force development in permeabilized myocytes (Fig. 1). The donor and rToF-PVR permeabilized myocytes used in the functional experiments had similar cross-sectional areas: 395 ± 66 μm^2 vs 411 ± 57 μm^2, for donor and rToF-PVR myocytes, respectively. For each myocyte, we first measured the passive stiffness of the myofilaments, as assessed by the increase in passive force upon sarcomere stretch from 2.0 µm to 2.3 µm. There was some variability between the passive stiffnesses of the permeabilized myocytes within and between patient samples, but overall there was no significant difference in passive stiffness between the rToF-PVR and donor myocytes (Fig. 1B), with passive forces of 5.36±1.82 $kN.m^{-2}$ (n=6 patients) and 4.83±2.23 $kN.m^{-2}$ (n=7 donors; P = 0.65, unpaired t-test of patients *vs* donors), respectively.

Following the passive stiffness measurements, the myocytes were activated with Ca^{2+} and their Ca^{2+}-activated contractile properties were studied, for the following key parameters: Maximum Ca^{2+} activated force (Fig. 1C) was 16.3±5.6 $kN.m^{-2}$ in rToF-PVR patients (n=7 patients) and 14.1±4.1 $kN.m^{-2}$ in RV donors (n=7 donors; P = 0.42). Crossbridge cycling kinetics, k_{tr}, at maximal Ca^{2+} (Fig. 1D) were 2.01±0.39 s^{-1} (n=7 patients) and 2.08±0.23 s^{-1} (n=7 donors; P = 0.70). The Ca^{2+} sensitivity of force

development (Fig. 1E), as quantified by the pCa_{50} value (Fig. 1F), was 5.80±0.19 (n=7 patients) and 5.80±0.20 (n=5 donors; P= 0.97). Thus none of these resting or Ca^{2+}-activated contractile parameters showed a difference between rToF-PVR patients and donors. From these results, we conclude that the contractile function of myofibrils in permeabilized myocytes from the rToF-PVR patients was similar to that in donor myocytes.

Collagen content was similar in rToF-PVR and RV Donor tissue.

Collagens I and III are the major ECM protein constituents in the heart and these, together with lysyl oxidase that cross-links the collagen, are known to be the main determinants of tissue stiffness.[22] Quantitative PCR for mRNA expression of genes coding for collagen I, collagen III and lysyl oxidase (COL1A2, COL3A1 and LOX, respectively) revealed that rToF-PVR tissue was comparable with RV donor (Fig. 2A-C). Direct assessment of tissue structure by picrosirius red showed no quantifiable difference between the collagen content of rToF-PVR and RV donor tissue under either brightfield or circular polarized light (Fig. 2D, 2E). The latter was used to visualize only the highly birefringent fibers and identify potential deleterious organization of collagen that occurs as the fibrotic scar matures. In this setting only the birefringent (bright) fibers are detected and indicate a predominance of collagen I over collagen III.[23]

Transcriptomic profiling revealed up-regulation of small leucine-rich proteoglycans in rToF-PVR

An Affymetrix human microarray was used to profile gene expression differences between heart tissue of rToF-PVR patients and RV donors. Principal component analysis, a multivariate analysis which places individual samples in 3-dimensional space relative to each other based on false discovery rate (q) and P-value, was performed. Application of thresholds (q=0.47 and P=0.004)

showed clear clustering of samples within groups and clear separation between rToF-PVR and RV donor samples (Fig. 3A) and yielded a list of 601 transcripts, of which 330 encoded known genes (Supplemental Table). Hierarchical clustering showed grouping by disease, with consistent groups of up- and downregulated genes that were evenly distributed (Fig 3B). Volcano analysis showed that the differentially-regulated genes carrying the greatest degree of statistical significance were downregulated in rToF-PVR myocardium (Fig. 3C). Gene Ontology (GO) pathway analysis clusters the differentially regulated transcripts by utilizing databases of gene names (or 'ontologies') based on known associations as found in the existing body of literature. Using this method we determined that 'connective tissue diseases', 'response to wounding', 'inflammation' and 'immune response' were top scoring terms i.e. ones with the lowest P value, within their categories (Diseases by biomarkers, GO Processes, Process networks and pathway maps respectively) (Fig. 4). Visualization of the top 'Pathway Map' - immune response_Lectin induced complement pathway - showed that the transcripts in these pathways were predominantly downregulated (Fig. 5).

Lists of the 10 most up- and down-regulated transcripts according to fold change (Table 3) showed that genes encoding asporin, lumican and osteoglycin, which are all members of the family of SLRP extracellular matrix proteins, were upregulated in rToF-PVR heart tissue compared with RV donor. Gene set enrichment analysis showed that 'ECM proteoglycans' displayed a modest enrichment of genes at the leading edges of the analysis and transcripts were equally distributed between up- and down regulation (Fig. 6).

SLRP gene expression is not corroborated by protein abundance in rToF-PVR myocardium

To check the transcriptomics data relating to SLRP expression, we employed qPCR, which confirmed that genes for asporin (ASPN), lumican (LUM) and osteoglycin (OGN) all underwent

significant increases in mRNA expression in rToF-PVR myocardium (Fig. 7A). We then investigated their expression at the protein level. Western blotting showed a band corresponding to the predicted 43 kDa molecular weight for asporin in rToF-PVR samples and showed a trend towards increased expression (P=0.07) compared with RV donor samples. Lumican expression was similar between the groups, whilst osteoglycin, which is expressed in pre- (~40 kDa) and post- (~20 kDa) processed forms,[24] was expressed heterogeneously within and between groups (Fig. 7B). Overall, changes in protein abundance of these SLRPs was absent, with the exception perhaps of asporin which showed a tendency towards an increase in rToF-PVR samples compared with RV donors, though this will need examining further.

Immunofluorescence co-staining for asporin and the myofilament protein marker, myomesin, showed that asporin was mainly localized to non-myocyte populations, but also appeared in the intercalated disc of the myocytes (Fig. 8). Subjectively, no obvious differences between cohorts were observed.

Discussion

This is the first investigation, to our knowledge, of myofilament function, tissue structure and mRNA expression in the RV myocardium of adult, or near-adult, rToF patients requiring pulmonary valve replacement. We found no differences in the passive stiffnesses or the active contractile properties of the myofilaments in rToF-PVR myocytes compared with those in RV myocytes from donor hearts. Whilst we discovered subtle molecular differences in the ECM that may indicate an early phase of tissue remodeling in the RV of rToF-PVR patients, overall the myocardium of rToF patients undergoing PVR replacement based on current clinical criteria appears not to have undergone

substantial remodeling at the cellular level, which should be beneficial for a successful post-operative recovery.

Functional assessment of rToF-PVR cardiomyocytes

Previous studies have established that chronic dilation of the left ventricle, such as that triggered by MI or aortic regurgitation, leads to major changes to the contractile apparatus within the myocytes. For example, the passive stiffness of left ventricular myocytes is increased, due to changes in the expression and phosphorylation of the structural protein titin (which links actin and myosin filaments in the myofibril).[10, 12] This would tend to increase the diastolic stiffness of the ventricle. The Ca^{2+}-sensitivity of the myofibrils is increased due to a reduced phosphorylation of the regulatory protein troponin-I,[10, 25] and this would tend to increase systolic contraction of the ventricle, while slowing diastolic relaxation. The right ventricle too can show disease-dependent alterations within the myocytes that can influence the contractile state. Permeabilized myocytes from patients with pulmonary arterial hypertension and RV heart failure exhibit increased passive stiffness and maximum Ca^{2+}-activated force production compared with donor myocytes, and these changes could contribute to RV diastolic dysfunction in pulmonary arterial hypertension.[26, 27] To our knowledge, there have been no similar studies on the functional properties of myocytes from the volume-overloaded RV tissue of rToF patients, taken at the time of PVR surgery. We found no difference in passive stiffness of rToF-PVR permeabilized cardiac myocytes, compared with myocytes from non-diseased RV tissue (Fig. 1). Similarly, the steady-state properties (maximum force production, Ca^{2+} sensitivity) and dynamic properties (k_{tr}) of the myocytes during Ca^{2+} activation were the same as with the RV donor controls. Thus, we did not find any of the pathological changes in myofibrillar function that have been seen previously in volume-overloaded LV or in pressure-overloaded RV. This suggests

that the rToF-PVR myocytes we studied were structurally sound and that any structural remodeling of the myocytes had not occurred or had not reached a pathological state detectable by our experiments. In summary, these myocytes were essentially 'normal' and did not display a functional phenotype that has been associated with a severely diseased ventricle. Supporting this conclusion, although the RV was severely dilated in these patients, the RV ejection fraction was within the normal range.

Subtle changes in the ECM of the remodeled myocardium in rToF-PVR patients

ECM remodeling in which collagen content is increased is a cardinal feature of HF, as studied in left ventricle.[28] We observed that collagen content of myocardium was similar between rToF PVR and RV donor myocardium (Fig. 2), which contradicts previous studies which showed apparent fibrosis by cardiac MRI.[29] This may reflect the differences in the selectivity of the two modes of imaging, since MRI techniques rely on contrast agents that are thought to target scarred, inflamed or remodeled areas, whereas picrosirius red staining very specifically detects collagen fibers. We discovered subtle changes in ECM gene expression in rToF-PVR tissue compared with donor RV tissue. Tissue microarray revealed that there were differences in gene expression between donor RV myocardium and rToF PVR myocardium in 601 transcripts when subjected to a p value threshold of $p<0.04$ and a q of 0.47. The selection of these thresholds was determined because samples became functionally grouped at this point. The gene list that was generated (Figure 4) revealed that 'connective tissue diseases' were well represented, implicating the ECM changes in diseased tissue. Moreover, 3 of the top 10 transcripts from genes known to encode proteins belonged to the family of small leucine-rich proteoglycans (SLRPs). GO analysis of our transcriptomics data showed that immune related processes were also strongly implicated and we hypothesized as to whether inflammation was

contributing to an ECM disease milieu. However, analysis of pathway maps confirmed that the overwhelming majority of the players in the immune pathways were downregulated (Figure 5), making this unlikely. A note of caution is required with regard to the interpretation of our gene ontology analysis since the q threshold of 0.47, is notably low and may have led to substantial false hits. However, this was unavoidable because stricter thresholds would have resulted in a very limited list of genes for GO analysis and our intention was to validate 'hits' which supported our hypothesis with further experimentation.

Proteoglycans are ECM-modifying proteins which regulate the manner in which the core components of the ECM, i.e. collagens, interact with each other and with the surface of cells .[30] They are highly negatively-charged molecules that can facilitate hydration of the extracellular spaces to form gel-like structures such as the glycocalyx on the outer surface of cell membranes, potentially behaving as an ECM lubricant.[31] The rheological properties of proteoglycans are important in determining the surface mechanical properties of tissue and there is a growing realization that dysregulation of proteoglycans may contribute to pathological remodeling of the myocardium . For example, decorin and biglycan become highly expressed in models of hypertrophy and heart failure, and are responsible for facilitating fibrillogenesis and fibrosis.[32]

We identified increased mRNA for the SLRPs asporin, lumican and osteoglycin in rToF-PVR myocardium. Of these three, only asporin displayed a tendency for increased abundance at the protein level in rToF-PVR samples. However, the functional significance of this is unclear at present, because little is understood about the role of asporin in the heart. Upregulation of asporin has been observed during ECM remodeling in a pig model of myocardial infarction,[33] but further work is required to establish the importance of asporin in right ventricle function. In conclusion, our study provides evidence that the myocardium of rToF PVR patients undergoing pulmonary valve

replacement shows very little disturbance to myofilament function, histological structure and protein abundance, whilst gene expression changes may be indicative of an early response to volume overloading in these patients but this requires further investigation.

Clinical perspectives

Current indications of PVR are based on results of non-invasive assessment, including volumetric and cardiac systolic function assessment with CMR imaging, clinical evaluation of symptoms and objective assessment of exercise capacity using cardiopulmonary exercising testing modality. However, it is difficult to predict which patients will most improve after PVR. In a previous study we found that younger patients (<17.5 years) undergoing PVR exhibited greater 1-year improvement of LV dynamics and exercise capacity than in older patients. We suggested that the better outcome post-PVR in the younger patients could be due to a more compliant, less "diseased" right ventricle, perhaps reflecting better myocardial protection at the time of primary repair and a shorter exposure to volume overload.[7] However, the present results, which were performed mostly on patients in the older age range, did not show evidence for substantial myocardial disease, at least at the cellular and ECM levels. Thus, in these patients, approximately 20 years after ToF repair and with severe pulmonary regurgitation, the contractile properties of the RV myofibrils and the ECM composition and structure were comparable to those in normal RV tissue. This suggests that the poorer outcome that we observed previously in the older patient group is unlikely to be due to a poorer reversibility of myocyte and ECM function. Thus, current clinically-based predictive indices used to inform timing of PVR may be fit for purpose and are unlikely to subject patients to the risk of irreversible adverse remodeling of the RV.

We did find subtle changes in the expression of ECM genes in the rToF-PVR patients. Whether these changes might signal the impending onset of detrimental changes in collagen structure and myofibril function remains a topic for future studies.

Limitations

One of the main study limitations is the small number of available patients and the small amount of tissue that could be obtained from each, which did not allow us to test for any correlation between myocyte/ECM properties and age at the time of PVR. A more extensive study will be needed to address this potential correlation. Another potential limitation comes from the source of the tissue samples in the RV. Of necessity, we could obtain tissue only from the RV infundibulum when removing excessive residual muscle bundles. Whilst there is the potential that these samples might not be representative of the whole RV myocardium, these tissue sites have been exposed to the same chronic volume overload as the other areas within the RV, so the properties of their myocytes and ECM might be expected to be representative of those throughout the whole RV. Finally, the rToF-PVR samples and the donor samples came from patients having different clinical histories and from two different countries (patients undergoing PVR in the UK; brain-dead patients maintained on life support in Australia). However, using the same donor samples as a reference tissue, many studies have discovered substantial changes in myofilament function in other types of RV or LV disease,[21] so we have confidence that our finding of no change in myofilament function between the donor and rToF-PVR samples is a valid result.

Acknowledgements

All research at Great Ormond Street Hospital NHS Foundation Trust and UCL Great Ormond Street Institute of Child Health is made possible by the NIHR Great Ormond Street Hospital Biomedical Research Centre. The views expressed are those of the authors and not necessarily those of the NHS, the NIHR or the Department of Health. The authors would also like to acknowledge the assistance of the King's College London Genomics Centre in performing the transcriptomics array.

Sources of Funding

Supported by British Heart Foundation project grant PG/11/9/28705 (to J.C.K., A.F., V.T.)

Disclosures

None

Supplemental Material

Supplemental table: Full list of genes retrieved by applying filtering thresholds of p=0.004 and q=0.47 for the rToF-PVR vs RV donor microarray

Affiliations

From the British Heart Foundation Centre of Research Excellence, King's College London, London, UK (D.B., S-J.H., S.C.B., M.A., H.L., J.B-B., M.M., J.C.K.); Guys and St Thomas' NHS Trust, London, UK (A.F.); Great Ormond Street Hospital NHS Trust, London, UK (A.F., V.T.; H.J.; P-K.T.); University of Sydney, Sydney, New South Wales, Australia (C.G.dR.).

References

1. Perry LW, Neill CA, Ferencz C. Eurocat working party on. Congenital heart disease. Perspective in pediatric cardiology epidemiology of congenital heart disease, the baltimore-washington infant study 1981-89. . Armonk, NY:: Futura; 1993; 1993:33-62.
2. Knott-Craig CJ, Elkins RC, Lane MM, Holz J, McCue C, Ward KE. A 26-year experience with surgical management of tetralogy of fallot: Risk analysis for mortality or late reintervention. *The Annals of Thoracic Surgery*. 1998;66:506-511
3. Discigil B, Dearani JA, Puga FJ, Schaff HV, Hagler DJ, Warnes CA, Danielson GK. Late pulmonary valve replacement after repair of tetralogy of fallot. *J Thorac Cardiovasc Surg*. 2001;121:344-351
4. Frigiola A, Redington AN, Cullen S, Vogel M. Pulmonary regurgitation is an important determinant of right ventricular contractile dysfunction in patients with surgically repaired tetralogy of fallot. *Circulation*. 2004;110:II153-II157
5. Gatzoulis MA, Balaji S, Webber SA, Siu SC, Hokanson JS, Poile C, Rosenthal M, Nakazawa M, Moller JH, Gillette PC, et al. Risk factors for arrhythmia and sudden cardiac death late after repair of tetralogy of fallot: A multicentre study. *Lancet*. 2000;356:975-981
6. Therrien J, Marx GR, Gatzoulis MA. Late problems in tetralogy of fallot--recognition, management, and prevention. *Cardiol Clin.* 2002;20:395-404
7. Frigiola A, Tsang V, Bull C, Coats L, Khambadkone S, Derrick G, Mist B, Walker F, van DC, Bonhoeffer P, et al. Biventricular response after pulmonary valve replacement for right ventricular outflow tract dysfunction: Is age a predictor of outcome? *Circulation*. 2008;118:S182-S190
8. Heng EL, Gatzoulis MA, Uebing A, Sethia B, Uemura H, Smith GC, Diller GP, McCarthy KP, Ho SY, Li W, et al. Immediate and midterm cardiac remodeling after surgical pulmonary valve replacement in adults with repaired tetralogy of fallot: A prospective cardiovascular magnetic resonance and clinical study. *Circulation*. 2017;136:1703-1713
9. Oosterhof T, van SA, Vliegen HW, Meijboom FJ, van Dijk AP, Spijkerboer AM, Bouma BJ, Zwinderman AH, Hazekamp MG, de RA, et al. Preoperative thresholds for pulmonary valve replacement in patients with corrected tetralogy of fallot using cardiovascular magnetic resonance. *Circulation*. 2007;116:545-551
10. Hamdani N, Kooij V, van Dijk S, Merkus D, Paulus WJ, Remedios CD, Duncker DJ, Stienen GJ, van der Velden J. Sarcomeric dysfunction in heart failure. *Cardiovasc Res*. 2008;77:649-658
11. Hutchinson KR, Stewart JA, Jr., Lucchesi PA. Extracellular matrix remodeling during the progression of volume overload-induced heart failure. *J Mol Cell Cardiol*. 2010;48:564-569
12. LeWinter MM, Granzier HL. Titin is a major human disease gene. *Circulation*. 2013;127:938-944
13. Frigiola A, Hughes M, Turner M, Taylor A, Marek J, Giardini A, Hsia TY, Bull K. Physiological and phenotypic characteristics of late survivors of tetralogy of fallot repair who are free from pulmonary valve replacement. *Circulation*. 2013;128:1861-1868
14. Johnson GL, Kwan OL, Handshoe S, Noonan JA, DeMaria AN. Accuracy of combined two-dimensional echocardiography and continuous wave doppler recordings in the estimation of pressure gradient in right ventricular outlet obstruction. *J Am Coll Cardiol*. 1984;3:1013-1018
15. Hoskins A, Jacques AM, Bardswell SC, McKenna WJ, Tsang VT, dos Remedios Cristobel G, Ehler E, Avkiran M, Watkins HC, Redwood CS, et al. Normal passive viscoelasticity but abnormal myofibrillar contractile function in patients with obstructive hypertrophic cardiomyopathy. *Journal of Molecular and Cellular Cardiology* 2010;49:737-745
16. Dyer EC, Jacques AM, Hoskins AC, Ward DG, Gallon CE, Messer AE, Kaski JP, Burch M, Kentish JC, Marston SB. Functional analysis of a unique troponin c mutation, gly159asp, that causes familial dilated cardiomyopathy, studied in explanted heart muscle. *Circ Heart Fail*. 2009;2:456-464
17. Gomez-Arroyo J, Mizuno S, Szczepanek K, Van Tassell B, Natarajan R, dos Remedios CG, Drake JI, Farkas L, Kraskauskas D, Wijesinghe DS, et al. Metabolic gene remodeling and mitochondrial dysfunction in

failing right ventricular hypertrophy secondary to pulmonary arterial hypertension. *Circ Heart Fail*. 2013;6:136-144
18. Kruger M, Kotter S, Grutzner A, Lang P, Andresen C, Redfield MM, Butt E, dos Remedios CG, Linke WA. Protein kinase g modulates human myocardial passive stiffness by phosphorylation of the titin springs. *Circ Res*. 2009;104:87-94
19. Messer AE, Bayliss CR, El-Mezgueldi M, Redwood CS, Ward DG, Leung MC, Papadaki M, Dos Remedios C, Marston SB. Mutations in troponin t associated with hypertrophic cardiomyopathy increase ca(2+)-sensitivity and suppress the modulation of ca(2+)-sensitivity by troponin i phosphorylation. *Arch Biochem Biophys*. 2016;601:113-120
20. Zhang P, Kirk JA, Ji W, dos Remedios CG, Kass DA, Van Eyk JE, Murphy AM. Multiple reaction monitoring to identify site-specific troponin i phosphorylated residues in the failing human heart. *Circulation*. 2012;126:1828-1837
21. Dos Remedios CG, Lal SP, Li A, McNamara J, Keogh A, Macdonald PS, Cooke R, Ehler E, Knoll R, Marston SB, et al. The sydney heart bank: Improving translational research while eliminating or reducing the use of animal models of human heart disease. *Biophys Rev*. 2017;9:431-441
22. Lopez B, Gonzalez A, Hermida N, Valencia F, de Teresa E, Diez J. Role of lysyl oxidase in myocardial fibrosis: From basic science to clinical aspects. *Am J Physiol Heart Circ Physiol*. 2010;299:H1-9
23. Whittaker P, Kloner RA, Boughner DR, Pickering JG. Quantitative assessment of myocardial collagen with picrosirius red staining and circularly polarized light. *Basic Res Cardiol*. 1994;89:397-410
24. Deckx S, Heymans S, Papageorgiou AP. The diverse functions of osteoglycin: A deceitful dwarf, or a master regulator of disease? *FASEB J*. 2016;30:2651-2661
25. Wolff MR, Buck SH, Stoker SW, Greaser ML, Mentzer RM. Myofibrillar calcium sensitivity of isometric tension is increased in human dilated cardiomyopathies: Role of altered beta-adrenergically mediated protein phosphorylation. *J Clin Invest*. 1996;98:167-176
26. Hsu S, Kokkonen-Simon KM, Kirk JA, Kolb TM, Damico RL, Mathai SC, Mukherjee M, Shah AA, Wigley FM, Margulies KB, et al. Right ventricular myofilament functional differences in humans with systemic sclerosis-associated versus idiopathic pulmonary arterial hypertension. *Circulation*. 2018;137:2360-2370
27. Rain S, Handoko ML, Trip P, Gan CT, Westerhof N, Stienen GJ, Paulus WJ, Ottenheijm CA, Marcus JT, Dorfmuller P, et al. Right ventricular diastolic impairment in patients with pulmonary arterial hypertension. *Circulation*. 2013;128:2016-2025, 2011-2010
28. Gonzalez A, Lopez B, Ravassa S, San Jose G, Diez J. The complex dynamics of myocardial interstitial fibrosis in heart failure. Focus on collagen cross-linking. *Biochim Biophys Acta Mol Cell Res*. 2019;1866:1421-1432
29. Yim D, Riesenkampff E, Caro-Dominguez P, Yoo SJ, Seed M, Grosse-Wortmann L. Assessment of diffuse ventricular myocardial fibrosis using native t1 in children with repaired tetralogy of fallot. *Circ Cardiovasc Imaging*. 2017;10
30. Chen S, Birk DE. The regulatory roles of small leucine-rich proteoglycans in extracellular matrix assembly. *FEBS J*. 2013;280:2120-2137
31. Rabelink TJ, van den Berg BM, Garsen M, Wang G, Elkin M, van der Vlag J. Heparanase: Roles in cell survival, extracellular matrix remodelling and the development of kidney disease. *Nat Rev Nephrol*. 2017;13:201-212
32. Christensen G, Herum KM, Lunde IG. Sweet, yet underappreciated: Proteoglycans and extracellular matrix remodeling in heart disease. *Matrix Biol*. 2019;75-76:286-299
33. Barallobre-Barreiro J, Didangelos A, Schoendube FA, Drozdov I, Yin X, Fernandez-Caggiano M, Willeit P, Puntmann VO, Aldama-Lopez G, Shah AM, et al. Proteomics analysis of cardiac extracellular matrix remodeling in a porcine model of ischemia/reperfusion injury. *Circulation*. 2012;125:789-802

Figures

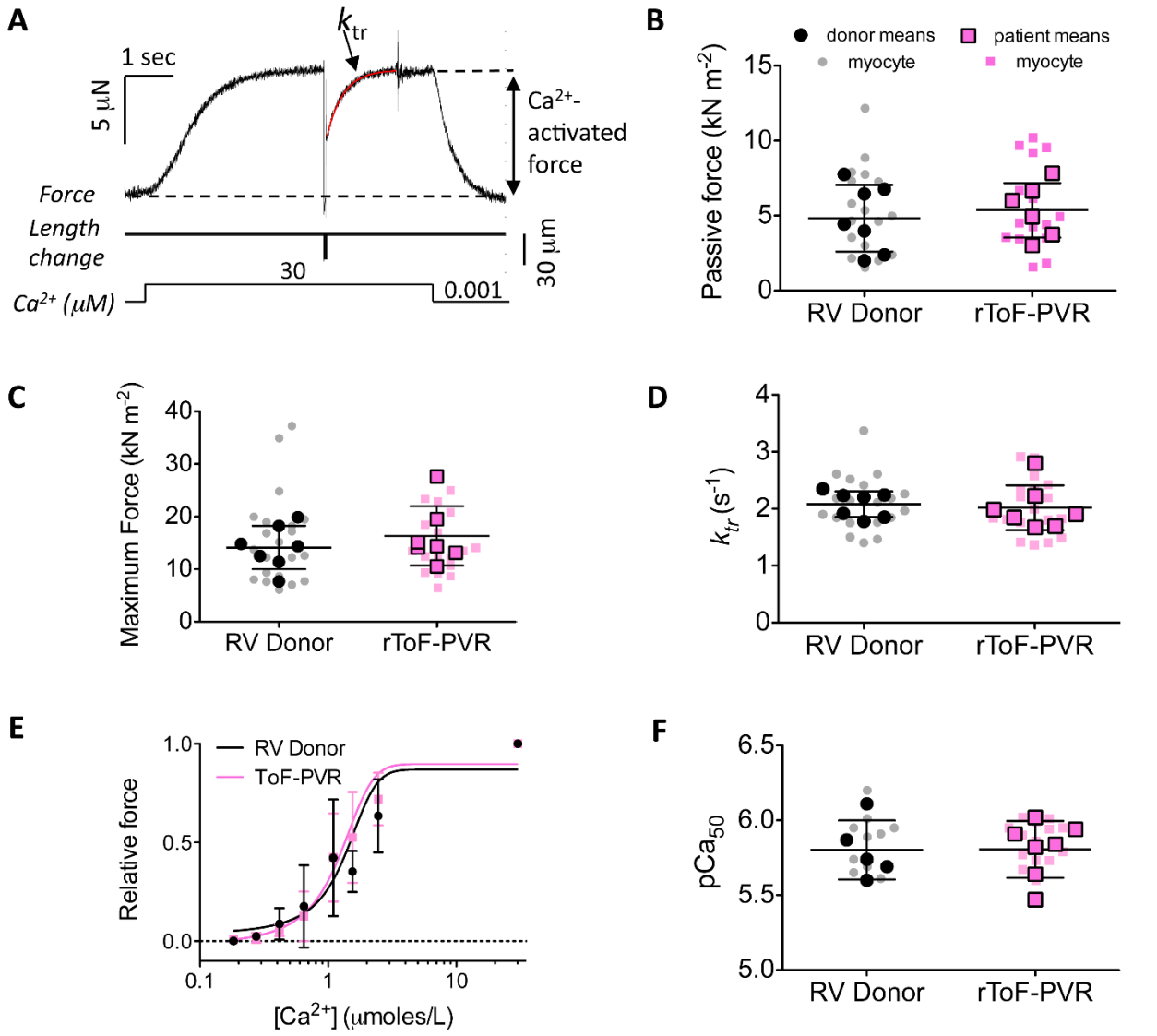

Figure 1. Passive stiffness and Ca^{2+} activated force in "permeabilized" cardiac myocytes from patients with Tetralogy of Fallot repair undergoing pulmonary valve replacement (rToF-PVR) are similar to those from right ventricle (RV) donors. A, A typical force trace showing activation of a single myocyte by an increase in solution Ca^{2+} and the measurement of Ca^{2+}-activated force and crossbridge kinetics (k_{tr}). For panels B-D & F each small symbol shows the result from one myocyte and each large symbol shows the mean derived from replicate myocytes from each donor or patient. The horizontal bars show the overall mean ± SD, calculated using each mean value derived from replicate myocytes (large symbols) as a single datum for the statistical analysis. **B,** Passive force, measured as the difference between passive forces at sarcomere lengths 2.0 µm and 2.3 µm. 19 RV donor myocytes (1-6 myocytes from each of 7 donors used in this panel), 16 rToF-PVR myocytes (1-4 myocytes from each of 6 rToF-PVR patients used in this panel). **C,** Maximum Ca^{2+}-activated force, corrected for myocyte cross-sectional area. 23 donor myocytes (1-6 myocytes from each of 7 donors), 19 rToF-PVR myocytes (1-4 myocytes from each of 7 patients). **D,** Rate of redevelopment of force (k_{tr}) after a release/restretch protocol at maximum Ca^{2+}. 21 donor myocytes (1-6 myocytes from each of

7 donors), 19 rToF-PVR myocytes (1-4 myocytes from each of 7 patients). **E,** Force-Ca^{2+} relationship. All forces are expressed relative to the maximum force at 30 µmol/L Ca^{2+}. In this panel the symbols show overall means ± SD for each [Ca^{2+}]. 1-6 myocytes from each of 5 donors, 1-4 myocytes from each of 7 patients. **F**, Ca^{2+} sensitivity, expressed as the pCa50 value: -log of [Ca^{2+}] required for 50% activation of force, and serves as a summary variable for the same data as in panel E. Statistical analysis showed no significant differences (*P*>0.05, unpaired t-tests) between the overall mean data for RV Donor and rToF-PVR patients for any of the measured parameters.

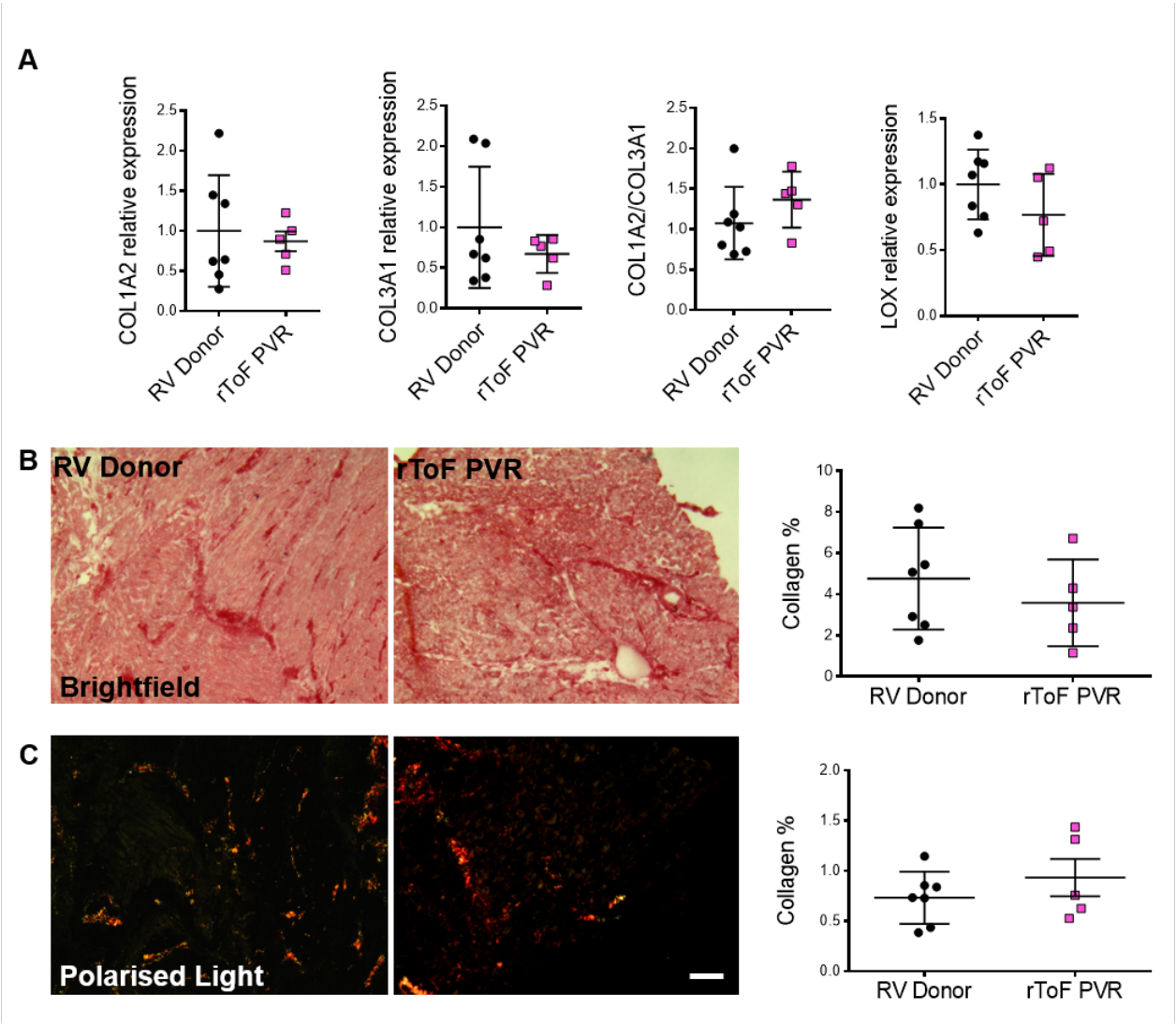

Figure 2. The collagen matrix in myocardium of patients with Tetralogy of Fallot repair undergoing pulmonary valve replacement (rToF-PVR) is similar to that in right ventricle (RV) donor myocardium. **A,** quantitative PCR analysis of mRNA expression for collagen I (COL1A2), collagen III (COL3A1) and lysyl oxidase (LOX) indicated no differences between rToF-PVR and RV donor myocardium. Each data point shows the result from one donor or rToF-PVR patient. **B,** Picrosirius red staining of collagen fibers in RV donor and rToF-PVR heart tissue sections with quantitation of the dark-red stained collagen fibers as a percentage of total tissue area. **C,** The same sections were viewed under polarized light to assess the presence of irreversibly linked collagen as a percentage of total tissue area. No statistical differences were observed between groups for all assays described. RV donor n=7, rToF PVR n=5. Values are expressed as mean ± SD. Scale = 30 µm.

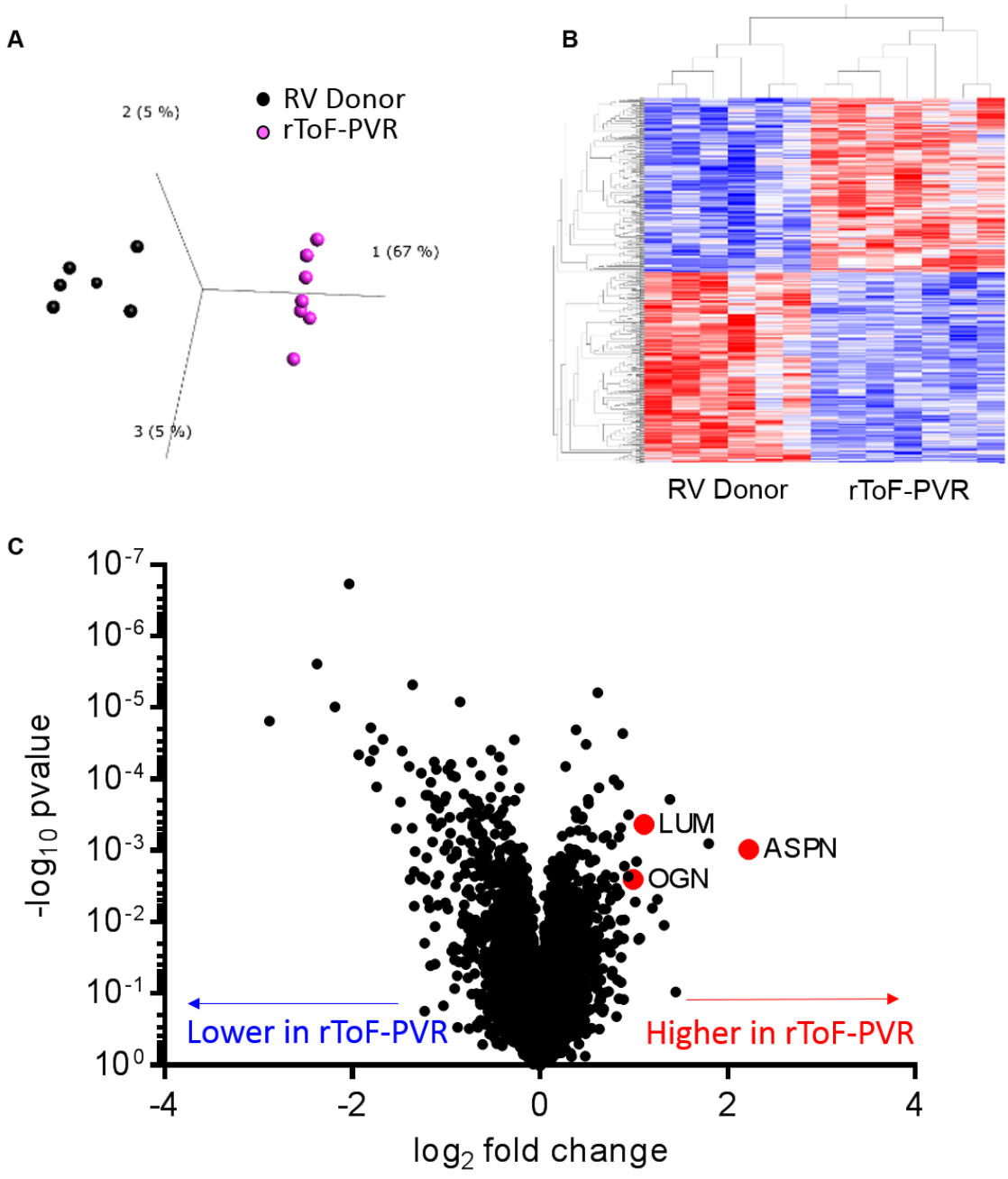

Figure 3. Analysis of the transcriptome identifies gene expression changes in myocardium of patients with Tetralogy of Fallot repair undergoing pulmonary valve replacement (rToF-PVR). A, Principal Component analysis of the gene expression profile of each tissue sample in relation to all others in the first 3 principal components revealed clear functional grouping of samples according to right ventricle (RV) donor (black) and rToF-PVR (magenta). Each data point shows the result from one RV donor or rToF-PVR patient. **B,** Hierarchical clustering also showed rToF-PVR samples were functionally grouped according to gene expression profile. Selected thresholds were a false discovery rate (q) of 0.47 and *P*=0.004. **C,** Volcano analysis revealed that the most profound differences occurred in downregulated genes. The transcripts ASPN, LUM and OGN were upregulated in rToF-PVR samples. Statistical measures applied to the dataset prior to analysis were a p value of 0.004 and a false discovery rate of 0.47. RV donor n=6, rToF-PVR n=7.

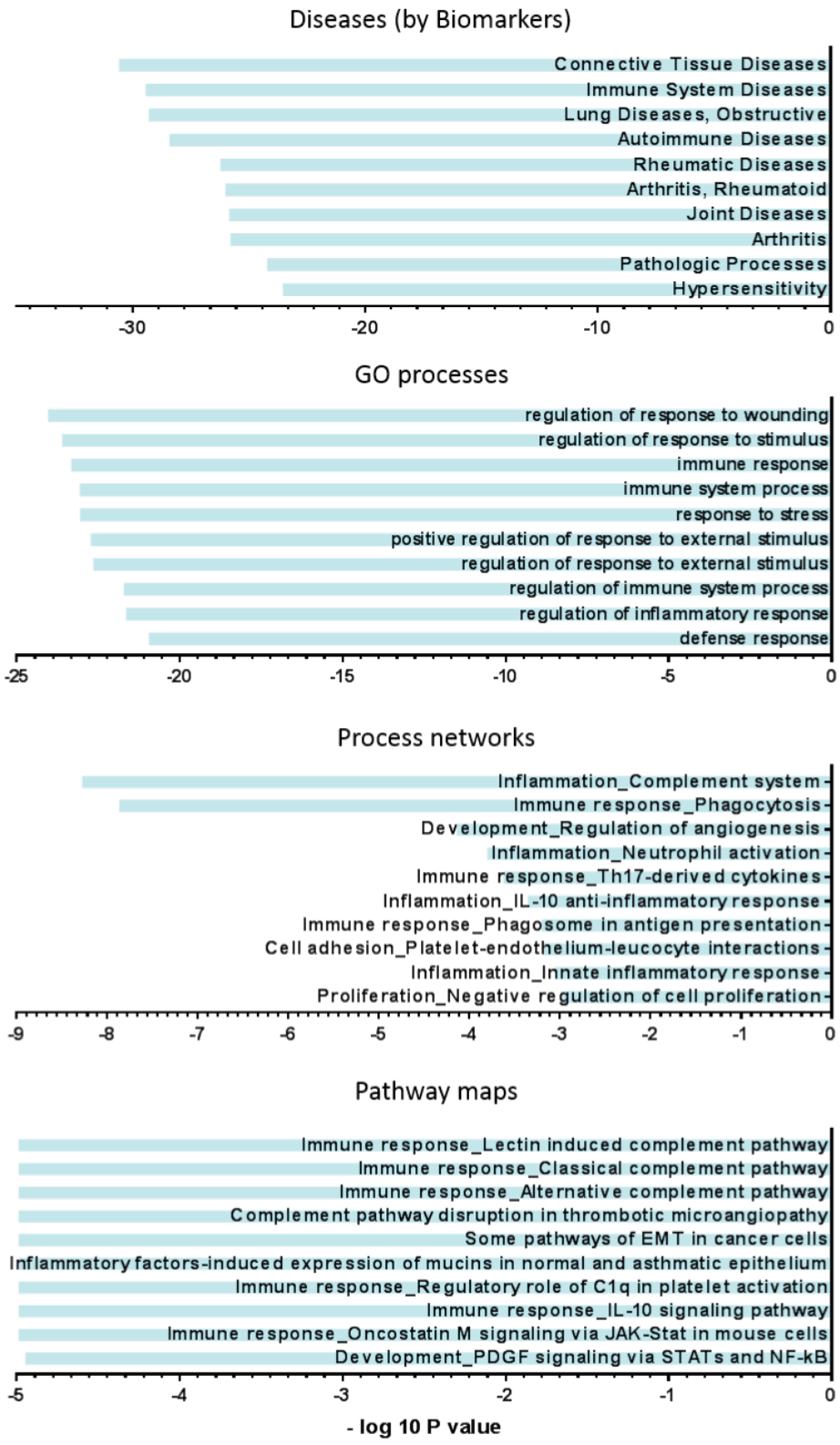

Figure 4. Gene ontology analysis implicated tissue remodeling and inflammation pathways as dysregulated in myocardium of patients with Tetralogy of Fallot repair undergoing pulmonary valve replacement (rToF-PVR). Holistic analysis of the differentially expressed genes in rToF-PVR myocardium compared with right ventricle donor against the gene ontology (GO) annotated database of affected biological processes ordered according to *P* value.

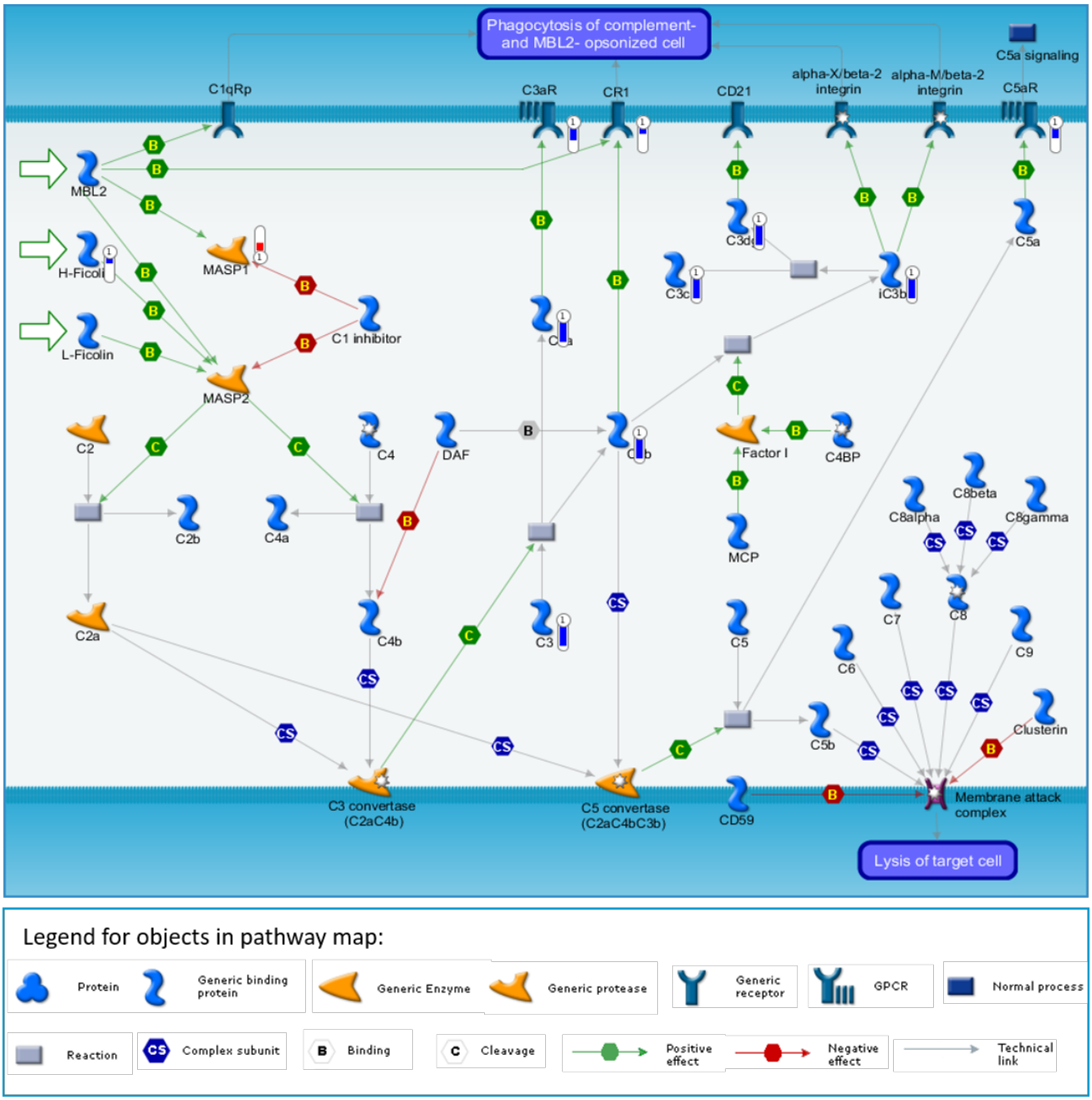

Figure 5. Schematic representation of the top scoring statistically significant pathway map indicated down regulation of genes involved in immune response in myocardium of patients with Tetralogy of Fallot repair undergoing pulmonary valve replacement. The top scoring map (map with the lowest p-value) based on enrichment distribution sorted by 'statistically significant maps' was Immune response_Lectin induced complement pathway. This shows negative regulation (blue thermomemeter) of most of the genes involved in this pathway implying suppression of immune pathways in rToF-PVR myocardium. Only one gene displayed upregulated expression (red thermometer). Many of the genes in the second and third top scoring maps overlapped with this map. The material in this figure is reproduced under a licence from Clarivate Analytics. You may not copy or redistribute this material in whole or in part without the written consent of Clarivate Analytics.

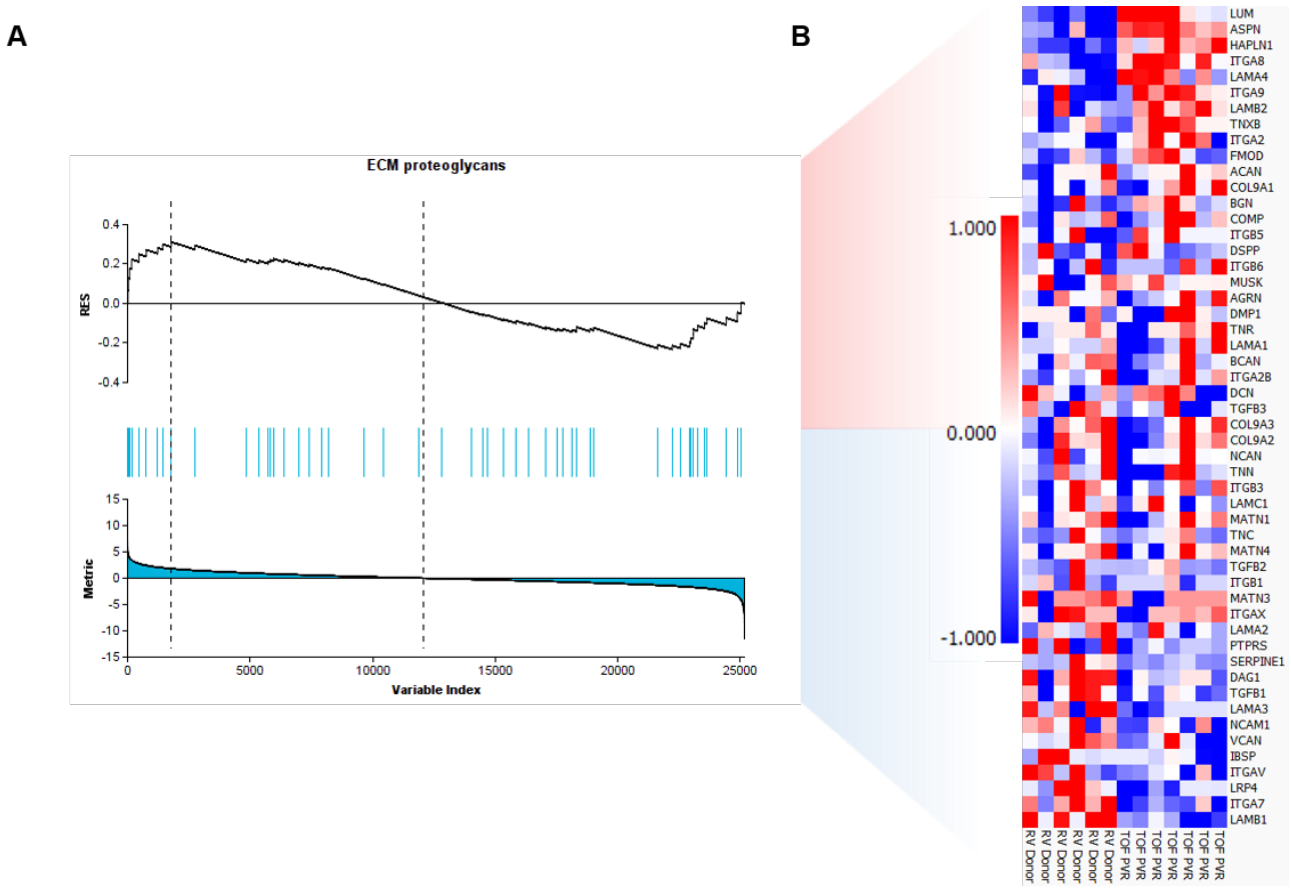

Figure 6. Gene set enrichment analysis showing the expression patterns of the Extracellular Matrix proteoglycan gene set in patients with Tetralogy of Fallot repair undergoing pulmonary valve replacement (rToF-PVR) compared with right ventricle (RV) donor myocardium. A, Gene Set Enrichment Analysis of extracellular matrix proteoglycans displaying some enrichment of genes at the leading edge. **B,** Corresponding heat map of genes and expression profiles for 6 RV donor samples and 7 rToF-PVR samples.

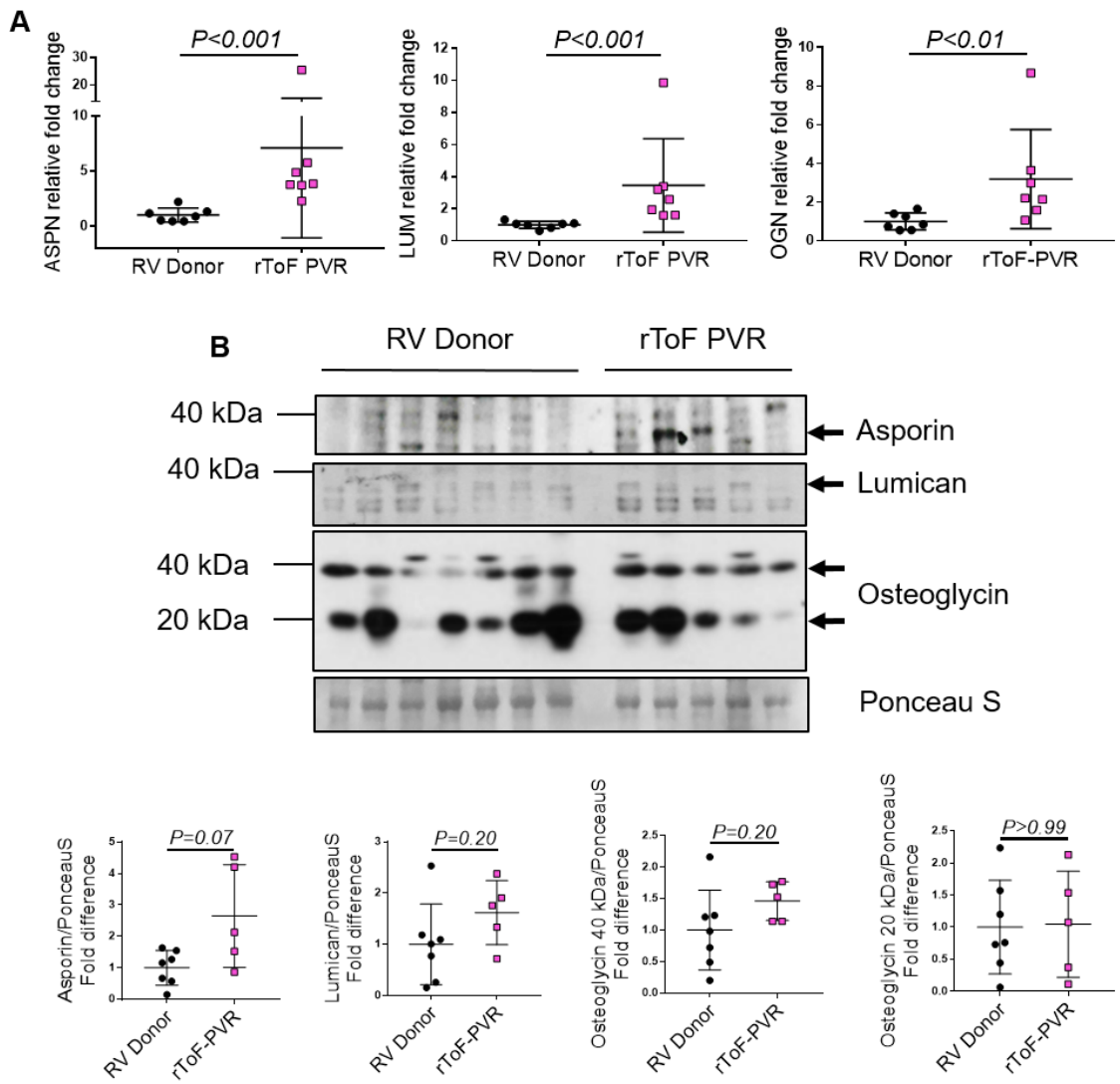

Figure. 7. **Validation of small leucine rich proteoglycan (SLRP) gene and protein expression shows asporin to be upregulated in several myocardial samples from patients with Tetralogy of Fallot repair undergoing pulmonary valve replacement (rToF-PVR). A,** mRNA validation of gene expression was performed by qPCR analysis for the genes encoding asporin (ASPN), lumican (LUM) & osteoglycin (OGN). n=7/group. Each data point shows the result from one right ventricle (RV) donor or rToF-PVR patient. Values expressed as mean ± SD, indicated p values were returned after performing Mann-Whitney U test. The p values were unchanged if the single rToF-PVR outlier was removed and the data analyzed using Student's unpaired t-test. **B,** Protein expression analysis for these genes was performed by Western blotting using antibodies probing for asporin, lumican, osteoglycin. Ponceau S shows equal loading of the gel lanes. Densitometry was performed for quantitation of protein abundance relative to ponceau S. n=7 RV Donor, 5 rToF-PVR. Values expressed as mean ± SD; *P* values were returned following Mann-Whitney U tests.

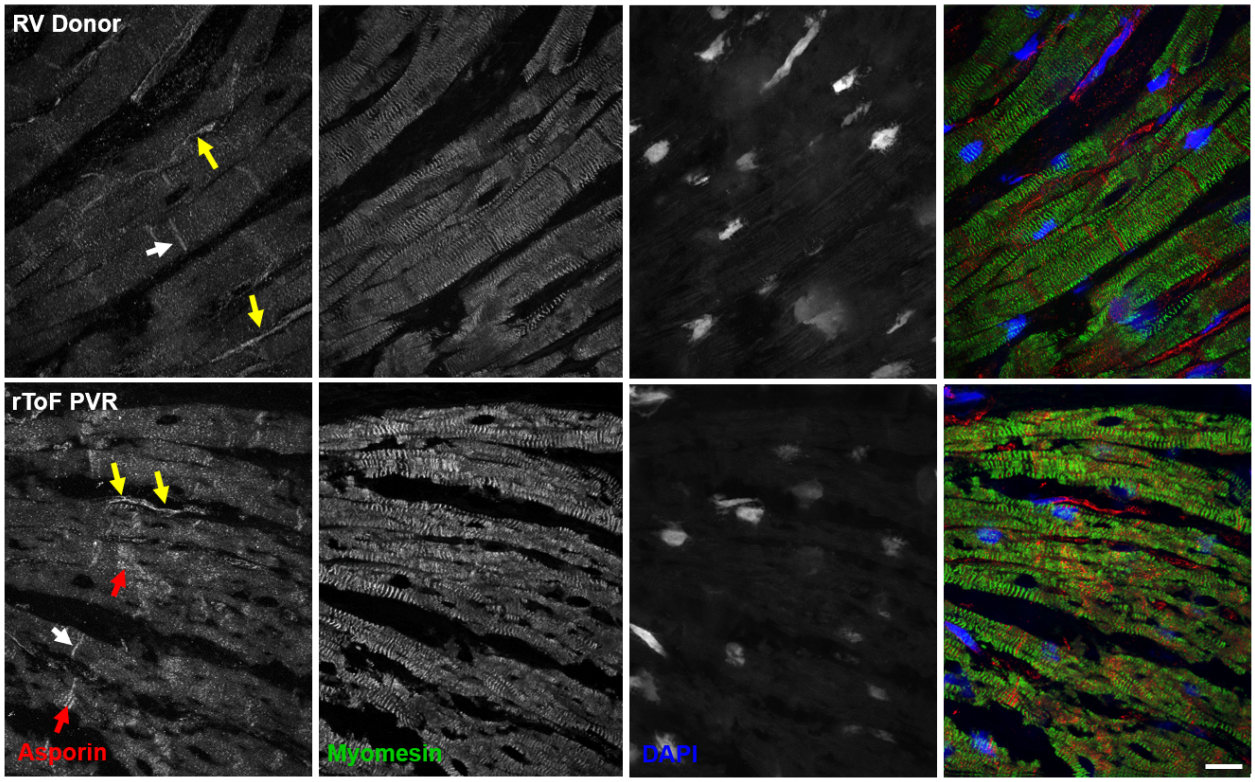

Figure 8. **Immunostaining of sections for asporin shows localization in extracellular domains and the intercalated disc in human right ventricle.** Asporin expression in right ventricle myocardium of both cohorts appeared in the extracellular domains in between the lateral membranes of cardiomyocytes suggestive of extraxcellular matrix localization (red arrows) or as regularly spaced bands indicative of intercalated disc staining (white arrows). Antibody to the sarcomere protein, myomesin, was used as a cardiomyocyte marker and DAPI was used to stain nuclear DNA. Scale bar = 10 µm.

Tables

Table 1. Primers used in this investigation used for qPCR

Gene	Forward	Reverse
ASPN	5' - CTC TGC CAA ACC CTT CTT TAG C - 3'	5' - CGT GAA TAG CAC TGA CAT CCA A - 3'
LUM	5' - TAA CTG CCC TGA AAG CTA CCC - 3'	5' - GGA GGC ACC ATT GGT ACA CTT - 3'
OGN	5' - TCT ACA CTT CTC CTG TTA CTG CT - 3'	5' - GAG GTA ATG GTG TTA TTG CCT CA - 3'
COL1A2	5' - GAG CGG TAA CAA GGG TGA GC - 3'	5' - CAC CCT GTG GTC CAA CAA CTC - 3'
COL3A1	5' - GGA GCT GGC TAC TTC TCG C - 3'	5' - GGG AAC ATC CTC CTT CAA CAG - 3'
LOX	5' - GCC GAC CAA GAT ATT CCT GGG - 3'	5' - GCA GGT CAT AGT GGC TAA ACT C - 3'
GAPDH	5' - GGA GCG AGA TCC CTC CAA AAT - 3'	5' - GGC TGT TGT CAT ACT TCT CAT GG - 3'

Table 2. Patients' characteristics: demographic, transthoracic echocardiogram (TTE), cardiopulmonary exercise testing (CPET) and cardiac MR imaging (CMR) data

	Patients (n=8)
Male:Female ratio	3:5
Age at repair (years)	2±2.6
Age at PVR (years)	24±12
NYHA	I (2), II (6)
TTE	
TAPSE (mm)	21±4
TR velocity (m/s)	2.5±0.4
RVOT peak velocity (m/s)	2.2±0.4
CPET	
Peak VO2 (ml/min/kg)	31±8
Peak VO2 % of predicted	84±11
VE/VCO2 slope	28±4
Peak HR (bpm)	180±13
CMR	
RV EDVi (ml/m^2)	149±26
RV ESVi (ml/m^2)	65±17
RV:LV EDV ratio	2.2±0.4:1
RV CO (L/m 2)	6.3±1.8
RV EF (%)	56±6
LV EDVi (ml/m^2)	71±19
LV EF (%)	66±7
LV CO (L/m 2)	3.5±0.4
PV RF (%)	48±7

PVR = pulmonary valve replacement; TAPSE=tricuspid annular systolic excursion; RV=right ventricle; LV=left ventricle; EDVi = end-diastolic volume indexed for body surface area; EF=ejection fraction; CO =cardiac output; PV RF=pulmonary valve regurgitant fraction

Table 3. The ten most up-regulated transcripts and ten most-downregulated protein coding transcripts

Gene Title	Gene Symbol	Difference	Fold change
Up-regulated transcripts			
asporin	ASPN	2.222	4.666
guanylate cyclase activator 1C	GUCA1C	1.799	3.481
frizzled-related protein	FRZB	1.383	2.608
lumican	LUM	1.108	2.156
natriuretic peptide receptor C/guanylate cyclase C (atrionatriuretic peptide receptor C)	NPR3	1.027	2.038
osteoglycin	OGN	0.9933	1.990
crystallin, mu	CRYM	0.9442	1.924
Fc fragment of IgE, high affinity I, receptor for; alpha polypeptide	FCER1A	0.899	1.865
fibronectin type III domain containing 1	FNDC1	0.881	1.842
endothelin receptor type A	EDNRA	0.845	1.797
Down-regulated transcripts			
RAS, dexamethasone-induced 1	RASD1	-1.672	0.313
V-set and immunoglobulin domain containing 4	VSIG4	-1.738	0.299
FK506 binding protein 5	FKBP5	-1.770	0.293
S100 calcium binding protein A9	S100A9	-1.800	0.287
coagulation factor XIII, A1 polypeptide	F13A1	-1.811	0.284
lymphatic vessel endothelial hyaluronan receptor 1	LYVE1	-1.929	0.262
phospholipase A2, group IIA (platelets, synovial fluid)	PLA2G2A	-2.035	0.243
serpin peptidase inhibitor, clade A (alpha-1 antiproteinase, antitrypsin), member 3	SERPINA3	-2.183	0.220
CD163 molecule	CD163	-2.373	0.192
metallothionein 1A	MT1A	-2.882	0.135